University of Groningen

X-ray photoemission spectroscopy study on the effects of functionalization in fulleropyrrolidine and pyrrolidine derivatives

Benne, Darja; Maccallini, Enrico; Rudolf, Petra; Sooambar, Chloe; Prato, Maurizio

IMPORTANT NOTE: You are advised to consult the publisher's version (publisher's PDF) if you wish to cite from it. Please check the document version below.

Document Version
Publisher's PDF, also known as Version of record

Link to publication in University of Groningen/UMCG research database

X-ray photoemission spectroscopy study on the effects of functionalization in fulleropyrrolidine and pyrrolidine derivatives

Darja Benne [a], Enrico Maccallini [a], Petra Rudolf [a,*], Chloé Sooambar [b], Maurizio Prato [b,*]

[a] *Materials Science Centre, Rijksuniversiteit Groningen, Nijenborgh 4, 9747 AG Groningen, The Netherlands*
[b] *Dipartimento di Scienze Farmaceutiche, Università di Trieste, Piazzale Europa 1, 34127 Trieste, Italy*

Abstract

Fulleropyrrolidine and pyrrolidine derivatives were studied using X-ray photoemission spectroscopy in order to determine the effects of the C_{60}-cage on the pyrrolidine nitrogen, as well as the influence of further derivatisation. Charge transfer from the carbon pyrrolidine ring to the C_{60}-cages is observed and this charge redistribution influences not only the carbon atoms but also the nitrogen. The major influence of different functionalization groups on the pyrrolidine nitrogen is whether or not they lead to quaternisation while no differences could be detected for different groups (methyl group or alkyl chain) producing one or the other configuration. However, the type of counter ion is important for the stability of the pyrrolidinium nitrogen: demethylated nitrogen, always found to be present in iodide counter balanced compounds, disappears in compounds counter balanced with BF_4^- anion.
© 2006 Elsevier Ltd. All rights reserved.

1. Introduction

C_{60} and its derivatives are of high technological interest because of their outstanding photophysical [1] and electrochemical [2] properties. Among the wide variety of organofullerene compounds, fulleropyrrolidine derivatives, which are characterised by the presence of a pyrrolidine ring fused to a 6,6 ring-junction of C_{60}, play an important role owing to their easy preparation with many possible synthetic variations [3]. Furthermore, mono-functionalization of C_{60} does not considerably alter the basic fullerene properties [2–4]. Thus, retaining the fullerene properties and having the advantage of possessing higher solubility in polar solvents fulleropyrrolidine derivatives are applicable in several

biological [5–7] and technological areas [8–12]. For example fulleropyrrolidine derivatives which possess positively charged groups are suitable compounds for the intercalation into aluminosilicates such as smectite clays [13]. Chemical modification of fullerenes is also useful for grafting them onto surfaces. In this way fulleropyrrolidine derivatives may play a relevant role in the design of novel molecular electronic devices [11].

The pyrrolidine nitrogen atom is located close to the fullerene sphere and as a consequence its chemical properties are affected to some extent. There are only a few studies on how the fullerene substituent modifies the chemical properties of groups linked to it [14,15]. The substituent effect on hydrophobic parameter, the basicity and nucleophilicity of fulleropyrrolidines was studied [16]. On the other hand additional groups fused to the pyrrolidine nitrogen atom also have an influence on the chemical properties of the pyrrolidine nitrogen atom. In the present work we want to study two different aspects: firstly the influence of the

---

* Corresponding authors. Tel.: +31 50 363 4736; fax: +31 50 363 4879 (P. Rudolf); tel.: +39 040 558 7883; fax: +39 040 52572 (M. Prato).

E-mail addresses: p.rudolf@rug.nl (P. Rudolf), prato@univ.trieste.it (M. Prato).

fullerene sphere and secondly the influence of further derivatisation on the properties of the pyrrolidine nitrogen by X-ray photoelectron spectroscopy (XPS).

XPS is an ideal tool for this purpose because XPS spectra can be used to obtain information about the chemical bonding by comparing the binding energies of the same atom in different environments. XPS enables us to understand the bonding interaction of fulleropyrrolidines in the solid state and the influence of the fullerene sphere and further functionalization on the pyrrolidine nitrogen atom.

The adsorption of pyrrolidine on silicon surfaces has been studied by XPS [17,18], however, there are no XPS data on its derivatives in the literature. Fulleropyrrolidine-derivative assembled as Langmuir–Blodgett films have been studied by XPS [19,20]. Here we extend these studies in a systematic way to various compounds and their chemical modification and functionalization including different nitrogen groups. The molecules studied are listed in Table 1 and their chemical structure in Fig. 1.

Table 1
Name and characteristic of the compounds studied

| Number	Name	Notes
1	*N*-Methylpyrrolidine	–
2	*N,N*-Dimethylpyrrolidinium iodide	–
3	*N*-Methylfulleropyrrolidine	Fullerene compound analogue of **1**
4	*N,N*-Dimethylfulleropyrrolidinium iodide	Fullerene compound analogue of **2**
5	*N*-mTEGfulleropyrrolidine	With a triethylene glycol mono-methyl ether (mTEG) long side chain
6	*N*-Methyl-*N*-mTEGfulleropyrrolidinium iodide	The methylated salt of **5** with iodide counterion
7	*N*-Methyl-*N*-mTEGfulleropyrrolidinium tetrafluoroborate	The methylated salt of **5** with tetrafluoroborate counterion
8	*N*-(3,6-Dioxaoctan-1-*tert*-butoxycarbonyl-amine)-fulleropyrrolidine	Boc protected secondary amine end function
9	*N*-(Methylfulleropyrrolidinium-1-yl-iodide)-3, 6-dioxaoctan-1-*tert*-butoxycarbonyl-amine	The methylated salt of **8** with iodide counterion
10	*N*-(Methylfulleropyrrolidinium-1-yl-iodide)-3, 6-dioxaoctan-1-ammonium trifluoroacetate	Ammonium trifluoroacetate end function
11	–	Ferrocene group close to the fulleropyrrolidine nitrogen; ammonium trifluoroacetate end function
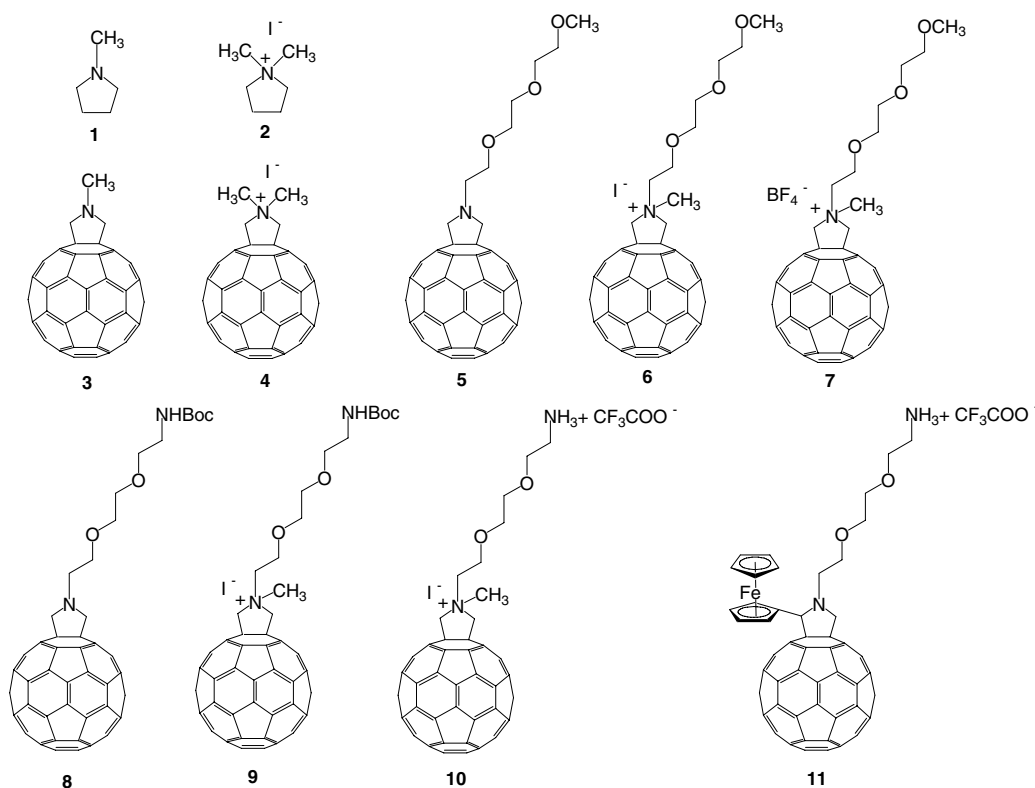
Fig. 1. Schematic drawings showing the chemical structure of fulleropyrrolidine and the pyrrolidine derivatives studied.

2. Experimental

2.1. General

The *N*-methylpyrrolidine (**1**) was obtained from Fluka Sigma–Aldrich. Compounds **2**–**6** and **8**–**11** were all prepared according to reported procedures in the literature [21–23]. Compound **7** was prepared as follows: 21 mg (0.020 mmol) of **6** was sonicated for 5 min in 5 mL of methanol and the insoluble material removed by centrifugation; to this brown solution of the fullerene salt **6** a solution of 78 mg (0.398 mmol, 20 equiv) of silver tetrafluoroborate, AgBF₄, dissolved in 2 mL of methanol was added dropwise. During the addition of the AgBF₄ solution a brown precipitate started to form in methanol. After 15 min a suspension of a brown precipitate in a clear solution of methanol was obtained. Methanol was then separated from the precipitate by centrifugation. Successively the brown solid was dissolved completely in dichloromethane (2 mL) and a white precipitate of AgI started to form. This precipitate was removed from the brown solution by centrifugation. This operation was repeated twice. Dichloromethane was evaporated under vacuum and then the brown solid was precipitated in hexane from a small amount of dichloromethane to yield the brown compound **7**.[1]

FT-IR spectra were recorded using KBr powder (DRIFT system). ¹H NMR spectrum was recorded at 200 MHz in CDCl₃. Chemical shifts are given in parts per million (δ) relative to tetramethylsilane. To collect ES-MS spectra, the compounds were dissolved in methanol.

2.2. Sample preparation

In this study, evaporated gold films supported on glass (Arrandee, Germany) were used as substrates. They were cleaned in an ozone discharge (UV-Ozone Photoreactor TM PR100, Ultra Violet Products) for 15 min and sonicated in ethanol for 20 min immediately before being employed. A 0.5–1% weight/volume of fulleropyrrolidine derivative suspension in water (or if not soluble in water in dichloromethane) was prepared. After sonication a small drop of the suspension was left to dry in air on the substrate. The pyrrolidine derivatives **1** and **2** were prepared in the same way to serve as reference samples.

Since the compounds are highly hygroscopic [24], all samples prepared from water suspension contain some water. In fact, the molecules decompose when heated and therefore cannot be dried completely. Even when introduced in UHV, the water does not desorb completely as evidenced by a typical water component at around 532.8 eV binding energy [25,26] that appears in all the O 1s photoemission spectra (not shown).

2.2.1. X-ray photoelectron spectroscopy

Samples introduced through a load lock system were measured using a SSX-100 (Surface Science Instruments) photoelectron spectrometer with a mono-chromatic Al-K$_\alpha$ X-ray source ($hv = 1486.6$ eV). The base pressure in the spectrometer was in the low 10^{-10} Torr range. The energy resolution was set to 1.16 eV to allow for an optimised combination of measuring time and resolution. The photoelectron take off angle was 37°. All binding energies of fulleropyrrolidine derivatives were referenced to the C 1s core level of the C₆₀-cage at 285.2 eV [27]. Binding energies of the pyrrolidine derivatives were referenced to saturated, non-functionalized carbon with a C 1s binding energy set at 285.0 eV. Spectral analysis included a background subtraction (Shirley background [28]), and peak separation using mixed Gaussian–Lorentzian functions [29], in a least squares curve-fitting program (WinSpec) developed at the LISE laboratory of the Facultés Uni-

versitaires Notre-Dame de la Paix, Namur, Belgium.[2] For the N 1s line, however, we had to employ a linear background subtraction since low peak intensity compared to the high secondary electron background following the substrate Au 4d peak did not allow for a reliable Shirley background subtraction.

During sample handling and data acquisition exposure to UV/vis light was avoided because the compounds are extremely unstable in UV/vis light. In addition, fluorine containing samples were sensitive to X-ray damage and measuring time had to be kept as short as possible for these samples.

3. Results and discussion

XPS spectra were taken for B 1s, C 1s, F 1s, Fe 2p, I 3d, N 1s and O 1s core levels. For each compound the spectra gave evidence for the presence of all elements associated with that compound and we observed binding energies and line-shapes (see below) consistent with the chemical structure and the stoichiometry.

3.1. Carbon 1s photoelectron line

We first discuss the carbon photoemission line to illustrate that the different functional groups can easily be identified with this technique.

3.1.1. Comparison of the N,N-dimethylpyrrolidinium iodide (2) with the N,N-dimethylfulleropyrrolidinium iodide derivative (4)

Compound **4** with the two methyl groups linked to the fulleropyrrolidine nitrogen is comparable to the pyrrolidine derivative **2** and hence suitable to study the influence of the fullerene sphere on the pyrrolidine.

C 1s photoemission lines of **2** and **4** are compared in Fig. 2. As shown in Fig. 2(a) for the pyrrolidine derivative **2**, the curve fitting procedure of this spectral region yields three peaks. The first peak at 285.0 eV binding energy is assigned to carbon atoms of the C–C bonds of the pyrrolidine ring not bound to nitrogen, while the second signal at 286.1 eV is arising from the nitrogen-bound carbons of the pyrrolidine ring and from the methyl carbons bound to nitrogen [30]. The latter peak is wider than the former because the two types of carbons contributing to it are not exactly equivalent. This assignment is supported by the intensity ratio of 1:2 between these two components. A third peak at 288.5 eV represents the contribution of CO_2 impurities due to air exposure of the film [31].

In the case of the fulleropyrrolidinium derivative **4**, analogue of **2** where the C₆₀-cage is present, the spectrum in Fig. 2(b) is observed. A large signal mainly due to the C₆₀-cage appears at 285.2 eV, however, it contains also
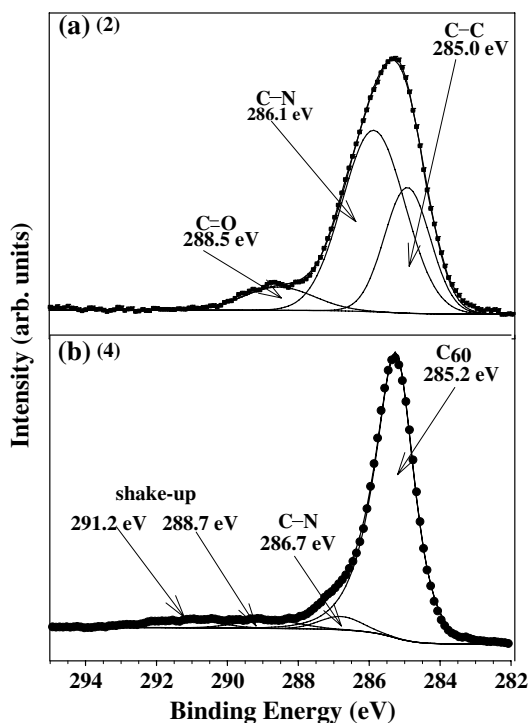

Fig. 2. X-ray photoemission spectra of the C 1s core level region for (a) *N*,*N*-dimethylpyrrolidinium iodide (**2**) and (b) *N*,*N*-dimethylfulleropyrrolidinium iodide (**4**).
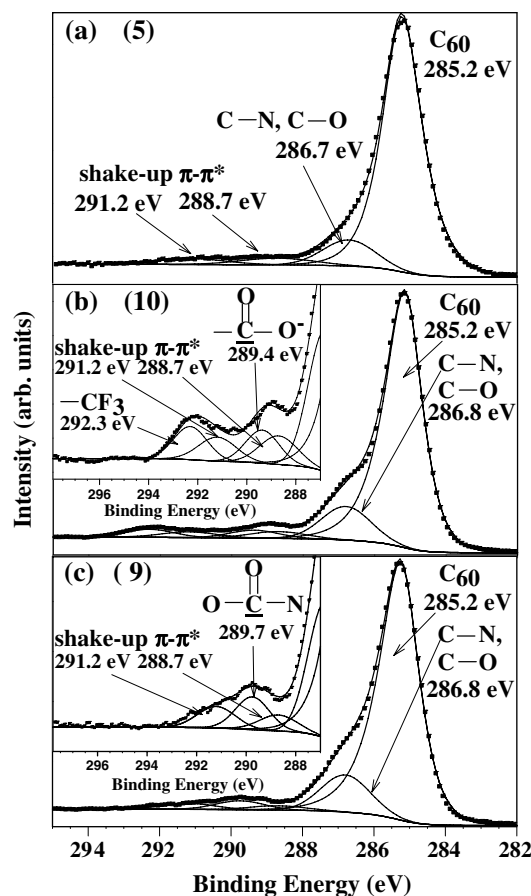

Fig. 3. X-ray photoemission spectra of the C 1s core level region for (a) *N*-mTEGfulleropyrrolidine (**5**), (b) *N*-(methylfulleropyrrolidinium-1-yl-iodide)-3,6-dioxaoctan-1-ammonium trifluoroacetate (**10**) and (c) fulleropyrrolidine derivative (**9**).

the contributions from the methyl groups close to the iodic ion and is slightly asymmetric compared to pure C_{60} [27]. In order to take this asymmetry into account in the peak fitting procedure we used a Losev peak shape [32]. The shake up features associated with the C_{60}-cage atoms are found at 288.7 and 291.2 eV [33]. The feature at 286.7 eV is due to the carbon atoms of the pyrrolidine ring bound to nitrogen. It is shifted 0.6 eV to higher binding energy compared to the spectrum of **2** indicating that a charge redistribution has occurred as a result of the functionalization. This interpretation is confirmed by the N 1s spectrum discussed below.

3.1.2. Fulleropyrrolidine derivatives possessing an oligoethylene glycol side chain

Further derivatisation of fulleropyrrolidines e.g. in the form of an alkyl tail fused to the pyrrolidine nitrogen atom make them suitable for grafting on surfaces such as modified electrodes [11]. The C 1s spectrum of compound **5** is displayed in Fig. 3(a). This spectrum clearly consists of four components. Here, only one signal at 286.7 eV is due to carbon atoms bound to nitrogen and carbon atoms single bound to one oxygen atom from the alkyl chain [30]. The binding energies of carbon bound to nitrogen and singly bound to oxygen are very similar [30,34] resulting in a broadened peak which, with our equipment, is not separable. The contribution due to carbon atoms of the C_{60}-cage and the corresponding shake up features are found at 285.2 eV, and at 288.7 and 291.2 eV [33], respectively, as for compound **4** discussed above.

3.1.3. Fulleropyrrolidines possessing a trifluoroacetate group

The C 1s spectrum of **10** is displayed in Fig. 3(b). At first look one identifies five peaks in the spectrum, however, close inspection reveals that the spectrum can be fitted only if one assumes at least six contributions: the first and most intense at 285.2 eV derives from carbon atoms of the C_{60}-cage and the corresponding shake up features are found at 288.7 and 291.2 eV; the spectral feature at 286.8 eV is due to carbon bound to nitrogen and oxygen; at 289.4 eV we have the contribution arising from of carboxylic carbon atoms and at 292.3 eV that of carbon bound to the more electronegative fluorine [30].

3.1.4. Fulleropyrrolidines possessing a secondary amine protected by a tert-butoxycarbonyl group (8, 9)

The C1s photoemission spectrum of **9** is presented in Fig. 3(c) together with the result of the curve fitting procedure which yields five peaks. The first peak at 285.2 eV is assigned to carbon atoms of the C_{60}-cage (with the associated shake up features at 288.7 and 291.2 eV) and to the methyl group. The second one at 286.8 eV is due to carbon atoms bound to oxygen and to nitrogen, while the third one at 289.7 eV arises from the contribution of carbamate carbon atoms [30].

From this analysis we can conclude that all functionalization groups of the various compounds can be identified in the C 1s region of the respective XPS spectrum. As a summary we include here the results of the curve fitting procedures of the C 1s lines of the various compounds in Table 2.

3.2. Nitrogen 1s photoelectron line

In this section we shall first examine the pyrrolidine nitrogen and show that the charge redistribution due to the presence of the C_{60}-cage influences not only the carbon atoms but also the nitrogen. The other major influence of different functionalization groups on the pyrrolidine nitrogen is whether or not a quaternisation occurs, while no differences can be detected for different groups (methyl group or alkyl chain) producing either configuration. In addition, we shall discuss the stability of end groups of the alkyl chain attached to the pyrrolidine nitrogen.

3.2.1. Comparison of the N,N-dimethylpyrrolidinium iodide (2) with the N,N-dimethylfulleropyrrolidinium iodide derivative 4

Recalling the short description of the compounds above, compound **4** is comparable to the pyrrolidinium derivative **2** and hence suitable to study the influence of the fullerene sphere on the binding energy of the pyrrolidine nitrogen atom. The N 1s region of the XPS spectra of **2** and **4** is depicted in Fig. 4(a) and (b), respectively. The N 1s photoelectron line of **2** is observed at 402.1 eV. When the C_{60}-cage is present (compound **4**), the binding energy increases by 1.0 eV to a value of 403.1 eV, indicating a decrease in the electron population around the nitrogen. This effect can be explained by a delocalisation of the nitrogen lone pair onto the fullerene core [14,16,35,36].

In the photoelectron spectra of both **2** and **4** a second peak with low intensity is observed at ~399.5 eV. This peak, arising from demethylated pyrrolidine nitrogen, is due to degeneration of the quaternary nitrogen counter balanced by iodide. In general, we have observed instability of iodide containing fulleropyrrolidines.

3.2.2. Fullerenes functionalized with a methylated pyrrolidinium nitrogen and an oligoethylene glycol chain

The addition of a longer alkyl chain on the pyrrolidine nitrogen atom enables the grafting of fullerene compounds
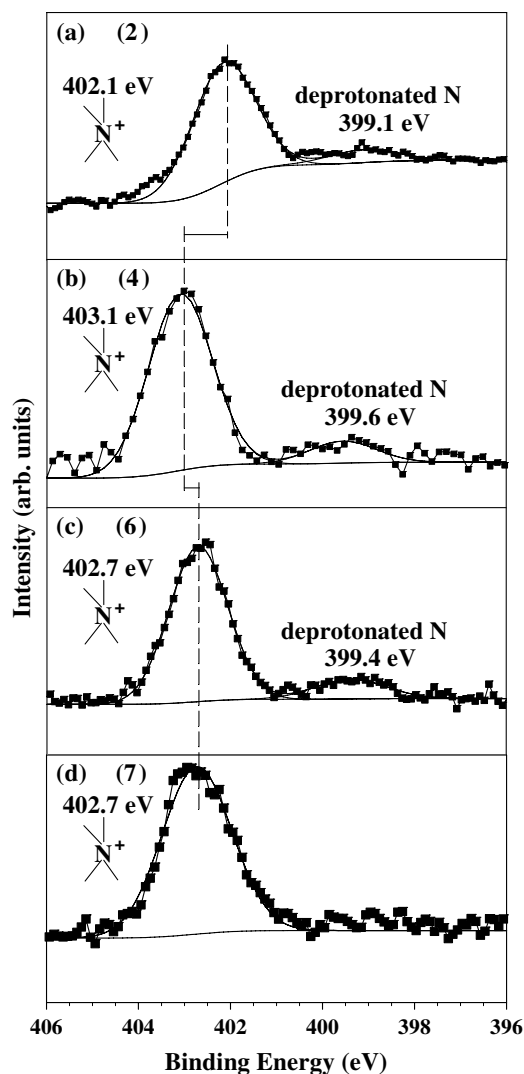

Fig. 4. X-ray photoemission spectra of the N 1s core level region for (a) N,N-dimethylpyrrolidinium iodide (**2**), (b) dimethylfulleropyrrolidinium iodide (**4**), (c) N-methyl-N-mTEGfulleropyrrolidinium iodide (**6**) and (d) N-methyl-N-mTEGfulleropyrrolidinium tetrafluoroborate (**7**).

on surfaces for applications such as modified electrodes [11]. We therefore focus on how this alkyl chain affects the binding energy of the pyrrolidine nitrogen atom. In Fig. 4(c) the N 1s region of the photoelectron spectrum of **6** is shown. The main peak is observed at a binding energy of 402.7 eV. This value is 0.4 eV lower than the one

Table 2
Binding energy, full width at half maximum and percentage of the total line area obtained from the fit of the C 1s core level emission spectra presented in Figs. 2 and 3

	Compound													
	2			**4**		**5**		**10**				**9**		
FWHM (eV)	1.6	2.0	2.5	*1.4	1.7	*1.4	1.8	*1.4	1.7	1.6	1.6	*1.4	1.7	1.6
E_b (eV)	285.0	286.1	288.5	285.2	286.7	285.2	286.7	285.2	286.8	289.4	292.3	285.2	286.8	289.7
Area (%)	30	60	10	92	8	87	13	79	15	3	3	82	14	4

Except the components marked with *, a Gaussian function line shape was used for all components used in the fit. Components marked with * were fitted with an asymmetrical function (Losev peak) and therefore the full width half maximum is calculated by doubling the distance from maximum height to half-height on the steep side [32].

observed for the same molecule without a long alkyl tail (**4**) and we attribute this difference to a variation in quaternisation of nitrogen present in the two molecules. In fact, quaternisation of nitrogen in $-NH_3^+$ increases the binding energy by ~1.5 eV [29] while quaternisation of amine gives rise to an upshift in binding energy of 2.5 eV [34]. However, we do not exclude that also differences in the position of the counter-ion influence the binding energy value.

Fullerene derivative **7** has the same functionalization as compound **6**. However, the pyrrolidinium nitrogen is balanced by a different counterion, the tetrafluoroborate (BF_4^-). The N 1s region is shown in Fig. 4(d). The binding energy value of 402.7 eV is exactly the same as the one determined for compound **6**. Thus, the change in the counter ion of the methylated pyrrolidinium nitrogen from iodide to BF_4^- has no effect on the binding energy value of the nitrogen atom.

It is important to note that the change in counter ion to the BF_4^- anion has, however, an effect on the stability of the pyrrolidinium nitrogen: the low intensity peak observed at ~399.5 eV arising from demethylated nitrogen which is present in all iodide counter balanced compounds disappears. Even after exposure to UV/vis light the spectrum of compound **7** did not reveal the presence of degenerated nitrogen.

3.2.3. Fullerenes functionalized with a neutral fulleropyrrolidine nitrogen

In Fig. 5(a) and (b) the *N*-methylfulleropyrrolidine (compound **3**) is compared with the fulleropyrrolidine functionalized with a long alkyl tail and a ferrocene group (compound **11**). The ferrocene group is an electroactive group widely used in fullerene chemistry to favour electron transfer processes from ferrocene to fullerene (see for example [37]). We thought it interesting to study by photoemission if there was any change in the nitrogen characteristics due to interaction with the ferrocene group. For the compounds **3** and **11** N 1s binding energy values of 399.8 and 399.7 eV are determined, respectively. The values are within the limit of error in good agreement and therefore, it can be concluded that the functionalization with a long alkyl tail on the fulleropyrrolidine nitrogen has no influence on the binding energy of this nitrogen. We can also deduce that the presence of the ferrocene group does not change the electron distribution around the fulleropyrrolidine nitrogen.
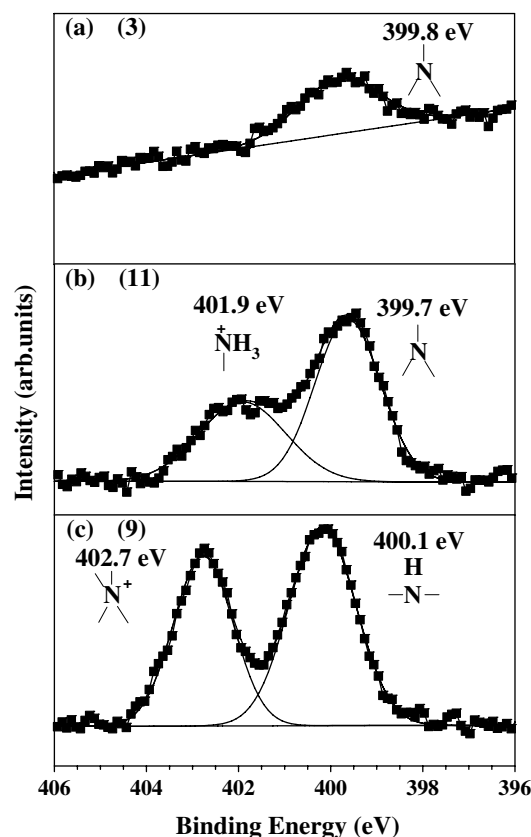

Fig. 5. X-ray photoemission spectra of the N 1s core level region for (a) *N*-methylfulleropyrrolidine (**3**), (b) fulleropyrrolidine derivative (**11**) and (c) *N*-(methylfulleropyrrolidinium-1-yl-iodide)-3,6-dioxaoctan-1-*tert*-butoxycarbonyl-amine (**9**).

As already mentioned in the introduction, fulleropyrrolidine derivatives possessing an ammonium end-group in the alkyl side chain are suitable for intercalation into silicate sheets [13]. We shall examine now their tendency to be subject to deprotonation. The second peak visible in the N 1s spectrum of compound **11** shown in Fig. 5(b) at a binding energy of 401.9 eV is due to the ammonium end group [38,39]. Based on the stoichiometry of the compound, one expects that the ratio between the N 1s intensities due to ammonium nitrogen and fulleropyrrolidine nitrogen to be 1:1. However, Fig. 5(b) reveals a much lower intensity ratio of ~0.5. The small intensity of the ammonium nitrogen contribution is due to its acidity. In fact, deprotonated amine nitrogen appears at a binding energy

Table 3
Binding energy, full width at half maximum and percentage of the total line area obtained from the fit of the N 1s core level emission spectra presented in Figs. 4 and 5

	Compound											
	2		**4**		**6**		**7**	**3**	**11**		**9**	
FWHM (eV)	1.6	1.6	1.6	1.6	1.6	1.7	1.7	2.0	2.1	1.7	1.6	1.7
E_b (eV)	402.1	399.1	403.1	399.6	402.7	399.4	402.7	399.8	401.9	399.7	402.7	400.1
Area (%)	90	10	89	11	87	13	100	100	40	60	43	57

A Gaussian function line shape was used for all components used in the fit.

of ~399.7 eV which overlaps with the peak due to the fulleropyrrolidine nitrogen.

3.2.4. Fulleropyrrolidines possessing a carbamate nitrogen

The alkyl tail is now functionalized with a primary amine protected by the *tert*-butoxycarbonyl (Boc) group instead of the ammonium trifluoroacetate group. In Fig. 5(c), the N 1s region of the spectrum of fulleropyrrolidine derivative **9** is depicted. One peak is observed at 402.7 eV arising from the methylated fulleropyrrolidine nitrogen (see section above), another peak at 400.1 eV is due to the carbamate nitrogen [40]. Compound **9** shows an almost ideal 1:1 ratio for the intensities of these two contributions, i.e. we have one fulleropyrrolidine nitrogen atom for each carbamate nitrogen atom.

For completeness, the results of all fitting procedures of the N 1s components discussed in Section 3.2 are summarised in Table 3.

4. Conclusion

The study of positively charged fullerene derivatives is relevant because fulleropyrrolidinium ions have interesting applications in photovoltaics [37,41,42]. In addition, amphiphilic compounds, such as those studied here, have appealing aggregation properties [43,44]. Photoemission spectroscopy gives evidence for charge transfer from the carbon pyrrolidine ring to the C_{60}-cages. This charge redistribution influences not only the carbon atoms but also the nitrogen. This technique also allows the identification of the different functional groups present in each molecule and indicates a charge redistribution in the pyrrolidine ring resulting from different functionalization depending on whether or not a quaternisation of the pyrrolidine nitrogen occurs. However, whether a methyl group or an alkyl chain produces one or the other configuration does not seem to influence the charge redistribution. We also found that the type of counter ion influences the stability of the pyrrolidinium nitrogen: in molecules where iodide is the anion, demethylated nitrogen is always found to be present while none is detected for molecules with BF_4^- anion.

References

[1] Guldi DM. Fullerenes: three dimensional electron acceptor materials. Chem Commun 2000(5):321–7.

[2] Echegoyen L, Echegoyen LE. Electrochemistry of fullerenes and their derivatives. Acc Chem Res 1998;31(9):593–601.

[3] Prato M, Maggini M. Fulleropyrrolidines: a family of full-fledged fullerene derivatives. Acc Chem Res 1998;31(9):519–26.

[4] Foote CS. Photophysical and photochemical properties of fullerenes. Top Curr Chem 1994;169:347–63.

[5] Da Ros T, Prato M. Medicinal chemistry with fullerenes and fullerene derivatives. Chem Commun 1999(8):663–9.

[6] Jensen AW, Wilson SR, Schuster DI. Biological applications of fullerenes. Bioorg Med Chem 1996;4(6):767–79.

[7] Nakamura E, Tokuyama H, Yamago S, Shiraki T, Sugiura Y. Biological activity of water-soluble fullerenes. Structural dependence of DNA cleavage, cytotoxicity, and enzyme inhibitory activities including HIV-protease inhibition. Bull Chem Soc Jpn 1996;69(8): 2143–51.

[8] Geckeler KE, Samal S. Syntheses and properties of macromolecular fullerenes, a review. Polym Int 1999;48(9):743–57.

[9] Guldi DM, Prato M. Excited-state properties of C-60 fullerene derivatives. Acc Chem Res 2000;33(10):695–703.

[10] Imahori H, Sakata Y. Fullerenes as novel accepters in photosynthetic electron transfer. Eur J Org Chem 1999(10):2445–57.

[11] Prato M. [60]Fullerene chemistry for materials science applications. J Mater Chem 1997;7(7):1097–109.

[12] Segura JL, Martin N. Functionalized oligoarylenes as building blocks for new organic materials. J Mater Chem 2000;10(11):2403–35.

[13] Gournis D, Georgakilas V, Karakassides MA, Bakas T, Kordatos K, Prato M, et al. Incorporation of fullerene derivatives into smectite clays: a new family of organic–inorganic nanocomposites. J Am Chem Soc 2004;126(27):8561–8.

[14] Eiermann M, Haddon RC, Knight B, Li QC, Maggini M, Martin N, et al. Electrochemical evidence for through-space orbital interactions in spiromethanofullerenes. Angew Chem Int Ed Engl 1995;34(15): 1591–4.

[15] Knight B, Martin N, Ohno T, Orti E, Rovira C, Veciana J, et al. Synthesis and electrochemistry of electronegative spiroannelated methanofullerenes: theoretical underpinning of the electronic effect of addends and a reductive cyclopropane ring-opening reaction. J Am Chem Soc 1997;119(41):9871–82.

[16] Bagno A, Claeson S, Maggini M, Martini ML, Prato M, Scorrano G. [60]Fullerene as a substituent. Chem-A Eur J 2002;8(5):1015–23.

[17] Cao XP, Coulter SK, Ellison MD, Liu HB, Liu JM, Hamers RJ. Bonding of nitrogen-containing organic molecules to the silicon(001) surface: the role of aromaticity. J Phys Chem B 2001;105(18):3759–68.

[18] Liu HB, Hamers RJ. An X-ray photoelectron spectroscopy study of the bonding of unsaturated organic molecules to the Si(001) surface. Surf Sci 1998;416(3):354–62.

[19] Giovanelli L, Le Lay G. A chemical and morphological study of fullerene derivatives Langmuir–Blodgett films. Appl Surf Sci 2000;162:513–8.

[20] Kang SZ, Xu SL, Han MJ, Lei SB, Wang C, Wan LJ, et al. Fabrication of a composite nano-ultrathin film of poly-phenylene–vinylene and C-60 derivative. Colloid Surf A 2005;257(58):195–8.

[21] Bosi S, Feruglio L, Milic D, Prato M. Synthesis and water solubility of novel fullerene bisadduct derivatives. Eur J Org Chem 2003:4741–7.

[22] Da Ros T, Prato M, Carano M, Ceroni P, Paolucci F, Roffia S. Enhanced acceptor character in fullerene derivatives. Synthesis and electrochemical properties of fulleropyrrolidinium salts. J Am Chem Soc 1998;120(45):11645–8.

[23] Kordatos K, Da Ros T, Bosi S, Vazquez E, Bergamin M, Cusan C, et al. Novel versatile fullerene synthons. J Org Chem 2001;66(14): 4915–20.

[24] Tenne R. Advances in the synthesis of inorganic nanotubes and fullerene-like nanoparticles. Angew Chem Int Ed 2003;42(42): 5124–32.

[25] Andersson K, Nikitin A, Pettersson LGM, Nilsson A, Ogasawara H. Water dissociation on Ru(001): an activated process. Phys Rev Lett 2004;93(19).

[26] Moulder JF, Stickle WF, Sobol PE, Bomben KD. Handbook of X-ray photoelectron spectroscopy. USA: Physical Electronics, Inc.; 1995.

[27] Maxwell AJ, Bruhwiler PA, Nilsson A, Martensson N, Rudolf P. Photoemission, autoionization, and X-ray-absorption spectroscopy of ultrathin-film C60 on Au(110). Phys Rev B 1994;49(15): 10717–25.

[28] Shirley DA. High-resolution X-ray photoemission spectrum of valence bands of gold. Phys Rev B 1972;5(12):4709–14.

[29] Briggs D, Seah MP. Practical surface analysis—Auger and X-ray photoelectron spectroscopy. Chinchester, UK: John Wiley; 1990.

[30] Beamson G, Briggs D. High resolution XPS of organic polymers—the Scienta ESCA300 Database. Chichester, UK: John Wiley & Sons Ltd.; 1992.

[31] Vogt AD, Han T, Beebe TP. Adsorption of 11-mercaptoundecanoic acid on Ni(111) and its interaction with probe molecules. Langmuir 1997;13(13):3397–403.

[32] Losev A. A new lineshape for fitting X-ray photoemission peaks. Surf Interface Anal 1989(14):845–9.

[33] Leiro JA, Heinonen MH, Laiho T, Batirev IG. Core-level XPS spectra of fullerene, highly oriented pyrolitic graphite, and glassy carbon. J El Spec Rel Phen 2003;128(2-3):205–13.

[34] Uchida E, Ikada Y. Introduction of quaternary amines onto a film surface by graft polymerization. J Appl Polym Sci 1996;61(8): 1365–73.

[35] Bianco A, Lucchini V, Maggini M, Prato M, Scorrano G, Toniolo C. *trans–cis* Amide bond isomerization in fulleroprolines. J Peptide Sci 1998;4(5):364–8.

[36] Brustolon M, Zoleo A, Agostini G, Maggini M. Radical anions of mono- and bis-fulleropyrrolidines: an EPR study. J Phys Chem A 1998;102(31):6331–9.

[37] Guldi DM, Luo CP, Koktysh D, Kotov NA, Da Ros T, Bosi S, et al. Photoactive nanowires in fullerene–ferrocene dyad polyelectrolyte multilayers. Nano Lett 2002;2(7):775–80.

[38] Cabibil HL, Pham V, Lozano J, Celio H, Winter RM, White JM. Self-organized fibrous nanostructures on poly[(aminopropyl)siloxane] films studied by atomic force microscopy. Langmuir 2000;16(26): 10471–81.

[39] Hooper AE, Werho D, Hopson T, Palmer O. Evaluation of amine- and amide-terminated self-assembled monolayers as 'Molecular glues' for Au and SiO$_2$ substrates. Surf Interf Anal 2001;31(9):809–14.

[40] Cecchet F, Pilling M, Hevesi L, Schergna S, Wong JKY, Clarkson GJ, et al. Grafting of benzylic amide macrocycles onto acid-terminated self-assembled monolayers studied by XPS, RAIRS, and contact angle measurements. J Phys Chem B 2003;107(39):10863–72.

[41] Guldi DM, Pellarini F, Prato M, Granito C, Troisi L. Layer-by-layer construction of nanostructured porphyrin–fullerene electrodes. Nano Lett 2002;2(9):965–8.

[42] Guldi DM, Prato M. Electrostatic interactions by design. Versatile methodology towards multifunctional assemblies/nanostructured electrodes. Chem Commun 2004(22):2517–25.

[43] Georgakilas V, Pellarini F, Prato M, Guldi DM, Melle-Franco M, Zerbetto F. Supramolecular self-assembled fullerene nanostructures. Proc Natl Acad Sci USA 2002;99(8):5075–80.

[44] Guldi DM, Zerbetto F, Georgakilas V, Prato M. Ordering fullerene materials at manometer dimensions. Acc Chem Res 2005;38(1):38–43.